Available online at www.sciencedirect.com

Chemical Engineering Research and Design

journal homepage: www.elsevier.com/locate/cherd

Surrogate model-based optimisation of a batch distillation process

Laszlo Hegely[*], *Ömer Faruk Karaman, Marton Tamas Szucs, Peter Lang*

Department of Building Sevices and Process Engineering, Faculty of Mechanical Engineering, Budapest University of Technology and Economics, Műegyetem rkp. 3., H-1111 Budapest, Hungary

ARTICLE INFO

Article history:
Received 19 December 2022
Received in revised form 14 February 2023
Accepted 24 February 2023
Available online 4 March 2023

Keywords:
Batch distillation
Simulation
Optimisation
Surrogate model
Waste solvent
Machine learning

ABSTRACT

A surrogate model-based method is proposed for optimising batch distillation processes and applied to the recovery of methanol from a five-component azeotropic waste solvent mixture, where pollutants are removed in two fore-cuts and an after-cut. The objective function is the profit of a single batch, while constraints are for the purity of the main cut and composition of the second fore-cut to be recycled. Simulations are performed by a flow-sheet simulator in a set of points in the space of optimisation variables (reflux ratios of steps, stopping criteria of fore-cuts). Algebraic surrogate models are fitted by ALAMO to simulation results to describe the objective function and the constraints. The resulting optimisation problem is solved numerically. The profit obtained is by 5% higher than the one previously obtained by genetic algorithm (commonly used for optimisation of batch distillation), while the number of simulations is reduced to its third. The highest profit, previously obtained by the Nelder-Mead simplex method, is approached within 1%. Although the simplex method required fewer simulations, the new method proposed here is a global one. The process is re-optimised for different prices to investigate their influence on the profit and optimal values of operational parameters.

1. Introduction

The treatment of waste solvent mixtures is frequently performed by batch distillation (BD) because of their varying amount and composition. These mixtures typically contain multiple organic components and water, which often form azeotropes. Components or azeotropes more volatile than the main component to be recovered can be removed in fore-cut(s), after which the main component is obtained in high purity as main cut. An after-cut can also be taken to remove either pollutants or the main component from the still residue. The off-cuts are either disposed of by incineration or recycled to a next batch to reduce the loss of the main component. Waste solvent regeneration is favourable both from an economic and an environmental point of view since it reduces both the amount of the fresh solvent to be purchased and that of the incinerated material.

By optimization, the profitability of BD processes can be increased, their energy demand and environmental impact can be decreased. For optimising BD processes, Mujtaba (2004) distinguished three optimisation problems: maximum distillate, minimum time and maximum profit. Minimising the time also decreases the energy demand. Other objective

Abbreviations: ALAMO, Automatic Learning of Algebraic Model; ANN, Artificial neural networks; BD, Batch distillation; DE, Differential evolution; GA, Genetic algorithm; LHS, Latin hypercube sampling; OF, Objective function; SMBO, Surrogate model-based optimisation; SM, Surrogate model; SQP, Sequential quadratic programming; VBA, Visual Basic for Application; VLE, Vapor-liquid equilibrium

* Corresponding author.
E-mail address: hegely.laszlo@gpk.bme.hu (L. Hegely).

https://doi.org/10.1016/j.cherd.2023.02.043

Nomenclature

A	acetone.
B	methanol.
C	THF.
Cr	stopping criteria, mass% or mass fraction.
D	water.
E	toluene.
m	mass, kg.
p	price, $/kg or $/t.
Q	heat duty, MJ/h.
r	heat of condensation, MJ/t.
R	reflux ratio.
t	duration of the process, h.
x	concentration, mass% or mass fraction.

Subscripts

1	first step (Fore-cut 1).
2	second step (Fore-cut 2).
3	third step (main cut).
4	fourth step (after-cut).
B	methanol.
C	THF.
d	(instantaneous) distillate.
E	toluene.
fc1	Fore-cut 1.
fc2	Fore-cut 2.
inc	incineration.
mc	main cut.
sr	still residue.
st	steam.

functions (OF) used include the energy demand (Furlonge et al., 1999) or the processing capacity (Nemeth et al., 2020) of the process, as well as environmental indicators such as CO_2 emissions (Wang et al., 2020), global warming and acidification potential (Zhao et al., 2021). As BD is a dynamic process, a dynamic optimisation problem must be solved. By the commonly used feasible path approach, the objective function is evaluated by solving the model of the process repeatedly at different points in the space of optimisation variables. However, simulation of the process is time-consuming. If a flow-sheet simulator is applied, the optimisation is most frequently performed by an external tool using an evolutionary (usually a genetic) algorithm (e.g. Pommier et al., 2008). Genetic algorithms are also commonly applied for multi-objective optimisation (Parhi et al., 2020). These methods require a large number of evaluations of the OF, making the optimisation computationally very intensive. Hegely and Lang (2016) maximised the profit of a conventional BD and a batch extractive distillation process by applying a genetic algorithm (GA). By both processes, methanol (B) was recovered from an azeotropic waste solvent mixture containing acetone (A), tetrahydrofuran (THF, C), water (D) and toluene (E), as well. The production campaign consisted of the regeneration of six batches with off-cuts recycled to the next batch.

As an alternative to computationally intensive evolutionary algorithms, direct search methods such as the Nelder-Mead simplex or Box-complex methods can be applied. Hegely (2023), taking as a case study the optimisation of the first batch of the conventional BD process studied by Hegely and Lang (2016), demonstrated that by the above-mentioned direct search methods, similar or even better OF values can be obtained as by GA with a much lower number (ca. by 80%) of simulations. A potential disadvantage of the Nelder-Mead simplex and Box-complex methods is that, being local optimisation methods, they can converge to a local optimum.

To make optimisation faster compared to evolutionary algorithms but without losing the ability to find a global optimum, a new surrogate model-based optimisation (SMBO) method is proposed here. Surrogate models (SMs) or metamodels are reduced models constructed from the inputs and outputs of rigorous models, whose evaluation is considerably less computationally intensive yet mimic the behaviour of the rigorous models. If SMs of OF (and eventually of the constraints) are available, an estimation of the real optimum can be rapidly obtained by finding the optimum of the surrogate OF. Several surrogate modelling techniques were applied recently for the optimisation of continuous distillation columns, such as kriging (Quirante et al., 2015), support vector machines (Jia et al., 2017) or artificial neural networks (ANN; Ibrahim et al., 2018). Although there are more and more works applying surrogate modelling for BD (e.g. Esche et al., 2022), SMBO of BD was only performed very few times. For such a dynamic optimisation problem, two different approaches can be distinguished. In the first one, SMs are used to describe the evolution of certain variables (e.g. concentration of the desired component in the distillate) in time. The optimisation, in this case, is still a dynamic optimisation problem, but the dynamic SMs are used to evaluate OF. Greaves et al. (2003) developed a dynamic SM to replace the rigorous one for the optimisation of a middle-vessel column. An ANN was trained with inputs of reflux and reboil ratios, distillate and bottom flow rates. The output vector consisted of the amount and composition of the distillate and the product in the middle vessel. The behaviour of the real plant was reproduced with good accuracy. The amount of products was maximised using sequential quadratic programming (SQP) with low computational effort. Khazraee et al. (2011) applied an adaptive neuro-fuzzy inference system to describe the evolution of the amount and composition of the distillate of a batch reactive distillation process. Optimisation was performed by differential evolution (DE); however, a questionable, dimensionally heterogeneous OF was used. The optimisation variables were the reflux ratio and the total batch time. In the second approach, SMs are fitted to the results of a large number of dynamic simulations, and the optimum of the surrogate OF is determined without a need for dynamic optimisation. Safe et al. (2013) studied a reactive distillation process in a batch dividing-wall column. A polynomial response surface was fitted to OF (the amount of ethyl acetate obtained in the distillate minus its amount lost in a side stream) as a function of the only two optimisation variables, the vapour and liquid split ratios. The optimum of the surface was then determined by DE. (It is not clear whether the presence of the dividing wall is advantageous.).

Additionally, the works of Mujtaba and Macchietto (1997) and Nemeth et al. (2020) must be mentioned. Nemeth et al. (2020) determined the optimal values of the optimisation variables and the objective function of a two-column process for different charge compositions by a GA. By fitting linear response surfaces to the results, it was possible to determine the optimum for any charge composition within the domain studied. However, this method cannot be truly considered an SMBO one since it first required performing the optimisation

using the rigorous model. The method of Mujtaba and Macchietto (1997), who solved the maximum profit problem for a reactive BD process, is only partially an SMBO one. First, the conversion of the limiting reactant was maximised for different batch times by SQP. The only optimisation variable was the (constant) reflux ratio. On the optimal reflux ratio and the calculated distillate amount, polynomial SMs were fitted as functions of the batch time. It was then possible to calculate the profit from the SMs, resulting in a surrogate optimisation problem, which can be solved with negligible computational effort. Although a dynamic optimisation problem must be solved first, the advantage of this method is that economic data only occurs in the profit function; therefore, only the surrogate optimisation problem has to be solved once again if cost parameters change. This highlights another advantage of SMBO: in contrast to conventional optimisation methods (such as GA) where the process has to be re-optimised if economic data change (Mujtaba and Macchietto, 1993), by SMBO, only the surrogate optimisation problem has to be solved once again, without any further simulation, provided the SMs are chosen appropriately, that is, they do not contain economic data. In fact, this is true for any parameters that are present in OF but do not affect simulation results.

To the best of our knowledge, the above literature review includes all the works on the application of SMs for the optimisation of BD processes. As it can be seen, non-dynamic SMs were only applied twice and with a very limited number (2) of optimisation variables, which constitutes the knowledge gap addressed in the present work.

The goal of this work is to propose a SM-based method for the fast optimisation of BD processes. In the space of the optimisation variables, a set of points is selected with Latin hypercube sampling (LHS). At each point, OF is evaluated by dynamic simulation with the professional flow-sheet simulator ChemCad, and algebraic SMs are fitted to the results by using ALAMO (Automatic Learning of Algebraic MOdel) software (Cozad et al., 2014). If necessary, the search space can be narrowed based on the results, and additional sampling can be performed. ALAMO is a machine learning tool that constructs algebraic models from predefined basis functions without the need to specify a function form a priori. The advantages of algebraic models are that they can be readily interpreted by humans, and their sensitivity to the input parameters is easy to calculate. To the best of our knowledge, ALAMO has not been previously used for the optimisation of distillation processes, although it has multiple advantages over other SM methods, according to Williams and Cremaschi (2021), who compared multiple methods. It had very good results in the optimisation of bowl-shaped functions, showed the most robust performance as the number of input dimensions was increased and had the lowest average optimisation time among the methods studied. The novelties of the present work are:

- non-dynamic SMs are applied to optimise a multicomponent, multistep BD process by considering all operational parameters for the first time,
- algebraic SMs are fitted to the simulation results of a BD process by using the ALAMO machine learning approach; the SMs used can provide a better fit than the polynomials applied by Safe et al. (2013),
- in order to evaluate the performance of the proposed method, its results are compared to those of two other methods.

The new optimisation method is applied to the case study of the methanol recovery by conventional BD previously optimised by a GA (Hegely and Lang, 2016; Hegely, 2023), the Nelder-Mead simplex and Box-complex methods (Hegely, 2023). The profit of the first batch of the campaign studied by Hegely and Lang (2016) is maximised. The effects of the price of methanol, incineration and heating steam on the optimal values of the operational parameters are also studied by SMBO. Additionally, different approaches to narrowing the search space are investigated.

The paper is structured in the following way. After the introduction, Section 2 describes the separation process. Section 3 presents the proposed SMBO approach, while the results are described in Section 4. Finally, conclusions and future research directions are discussed in Section 5.

2. Separation process

The waste solvent mixture to be treated contains 0.07 mass% acetone (A), 37.4% methanol (B), 4.89% tetrahydrofuran (C), 56.34% water (D) and 1.56% toluene (E). B must be recovered with a purity of 99.5%. Five minimum-boiling azeotropes are formed, in increasing order of boiling points: A-B, B-C, B-E, C-D and D-E. The azeotropes (except D-E) and A have lower boiling points than B. The recovery of B is hindered by the B-C and B-E azeotropes. (The concentration of A is very low, while the azeotrope C-D does not present a problem since C leaves earlier in a mixture of B and C.) Therefore, C and E must be removed in fore-cuts, causing a considerable loss of B. VLE calculations were performed by using the UNIQUAC model with the same binary interaction parameters used by Hegely and Lang (2016) and Hegely (2023) to make the results comparable. A more detailed description of the VLE is given in Hegely and Lang (2016).

The separation is performed in a distillation column with 27 theoretical plates (including the reboiler and the total condenser) (Hegely and Lang, 2016). The top of the column is at atmospheric pressure, while the total pressure drop is 0.25 bar. The volume of the charge is 25 m^3 (at 20 °C). The liquid hold-up of the condenser is 0.45 m^3, that of the column is 0.05 m^3/plate. The reboiler is heated with saturated steam of 3 bar (its heat of condensation is r_{st}=2263.5 MJ/t); its heat duty (Q_{st}) is1800 MJ/h.

The treatment of one batch consists of the following steps:

Step 0: heating-up of the column with total reflux in order to approach steady-state conditions. The step is finished after 360 min. At this point, the condensate contains mainly B and C, with a composition close to the azeotropic one.

Step 1: taking of the first fore-cut with a finite reflux ratio R_1 to remove the bulk C and E with a considerable loss of B. Fore-cut 1 is incinerated. Step 1 is finished when $x_{d,C} < Cr_1$ where $x_{d,C}$ is the instantaneous mass fraction of C in the distillate, and Cr_1 is the stopping criterion for Step 1.

Step 2: taking of the second fore-cut with reflux ratio R_2. This cut already contains B in a considerable concentration, but its pollutant (C and E) content is still too high. This cut is recycled to the next batch to limit the loss of B. This step is stopped when $x_{d,C} < Cr_2$.

Step 3: taking of the main cut (B product) with R_3. This step is finished (because of the increasing $x_{d,D}$) when $x_{mc,B} <$ 0.9952 where $x_{mc,B}$ is the mass fraction of B in the main cut. (Since, in the simulation, taking the main cut finishes only one time step (2 min) after the stopping criterion is

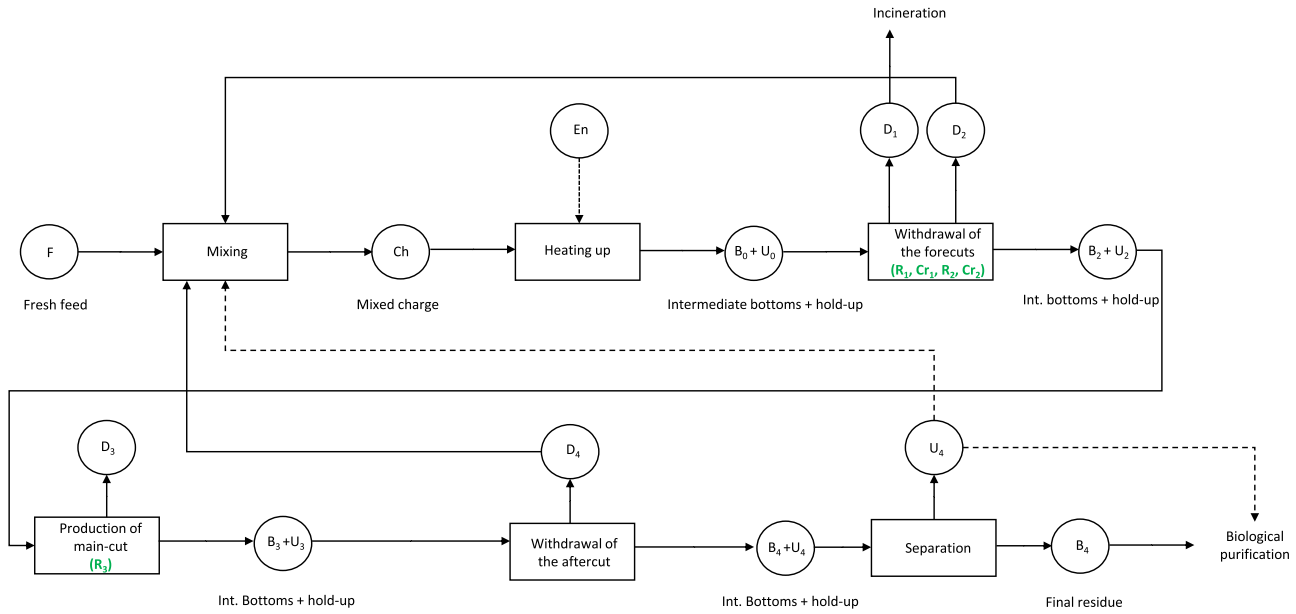

Fig. 1 – The state-task-network of the methanol regeneration process.

fulfilled, the value 0.9952 is used to ensure that $x_{mc,B}$ is actually close to 0.995.).

Step 4: taking of the after-cut with R_4. The aim of the after-cut is to remove B from the still residue so that it can be sent to biological purification. The after-cut has a considerable B content, and it is recycled to the next batch. Taking of the cut is finished when the B content of the still residue ($x_{sr,B}$) becomes lower than 0.25%.

A state-task-network is presented in Fig. 1. Rectangular boxes (states) represent the steps of the process, while the circles (tasks) represent the materials in the process. The hold-up of every third batch is sent to biological treatment, and the hold-up of other batches is recycled (dashed lines). Optimisation variables related to each step are indicated in green.

3. Calculation method

The objective function (OF; Eq. 1) is the profit of a single batch. It is composed of the price of methanol in the main cut, the costs of incineration of the Fore-cut 1 and of steam consumption during the process (Hegely and Lang, 2016).

$$OF = p_B m_{mc} - p_{inc} m_{fc1} - p_{st} \frac{Q_{st}}{r_{st}} t \quad (1)$$

where: p_B: price of methanol, 0.46 US$/kg, m_{mc}: mass of the main cut, kg, p_{inc}: price of incineration, 0.21 $/kg, m_{fc1}: mass of Fore-cut 1, kg, p_{st}: price of steam, 57.6 $/t, t: duration of the process, h.

The optimization problem is subject to the inequality constraints: Constraint 1: $x_{mc,B} \geq 0.995$, Constraint 2: $x_{fc2,C}/x_{fc2,B} \leq 0.107$, Constraint 3: $x_{fc2,E}/x_{fc2,B} \leq 0.12$, where $x_{fc2,B}$, $x_{fc2,C}$ and $x_{fc2,E}$ are the concentration of B, C and E in Fore-cut 2, respectively.

Constraint 1 guarantees the required purity of the product. Constraints 2 and 3 are needed to ensure that the organic pollutants C and E are not accumulated in Fore-cut 2 so that it can be recycled to the next batch. The numerical values in Constraints 2 and 3 are taken from the industrial practice. The optimisation variables are: R_1, R_2, R_3, and Cr_1, Cr_2. Since previous calculations showed that the effect of R_4 on OF is negligible, its value is kept constant at 5.41.

It can be assumed that in the optimum Constraints 2 and 3 are active, meaning that Fore-cut 2 contains the highest amount permitted of C and E. This is supported by previous results and can be explained by the fact that the part of C and E not present in Fore-cut 2 must be removed in Fore-cut 1, which would lead to a higher incineration cost. As shown later, this assumption proves to be true; however, it was not taken into account during the SMBO in order to not restrict the generality of the method.

In this work, a SMBO method is proposed (Fig. 2). First, a large number of test points are generated in the space of the optimisation variables by Latin hypercube sampling (LHS). In each point, simulation is performed by using ChemCad, whose results are the values of dependent variables necessary to calculate OF and the left-hand side of the constraints. If the number of feasible points (that is, where the constraints are not violated) is deemed sufficient for model fitting, surrogate models are generated by ALAMO; otherwise, the generation of test points is repeated by using a different (in this case, narrower) range of the optimisation variables.

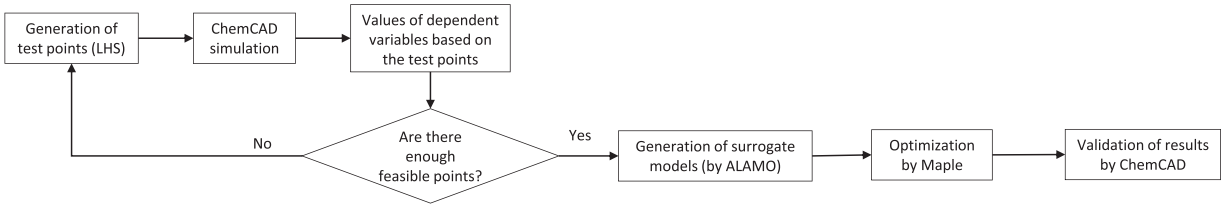

Fig. 2 – Flow chart of the surrogate model-based optimisation method.

Table 1 – Ranges of the values of the optimisation variables used for Latin hypercube sampling.

	R_1	R_2	R_3	Cr_1	Cr_2
Original range	1–10	1–10	1–5	0.10–0.30	0.015–0.050
Narrowed range	2–7	2–7	2–4.5	0.13–0.25	0.020–0.035

Optimisation of the surrogate OF is then performed in Maple. Finally, a simulation is performed with the values of the optimisation variables obtained to evaluate the difference of the OF values calculated by the SMs and by rigorous simulation. The smaller the difference, the better the fit of the SMs and the more likely that a good approximation of the true optimum is obtained. A detailed description of each step is given in the followings.

In order to obtain accurate SMs for the whole range of the optimisation variables, a more uniform sampling pattern than simple random sampling is preferred. In the space of the optimisation variables given in Table 1 as the original range, 500 points are generated by LHS. These ranges are selected based on previous calculation experience by Hegely and Lang (2016) and Hegely (2023) as well as on industrial practice. By LHS, the range of each variable is divided into 500 equal levels (intervals), thereby partitioning the space of the optimisation variables into 500^5 smaller hypercubes. From these, 500 are selected so that at each level, there is only one hypercube selected (Viana, 2016). Inside the hypercubes selected by LHS, the values of the optimisation variables are randomly generated with a uniform distribution.

Simulation is then performed at each point. The batch distillation process is modelled in ChemCad Version 7.1 in dynamic mode. The column is an SCDS module. The still pot and the accumulator tanks are DYNAMIC VESSELs. A DIVIDER is used to switch between the accumulators at the end of the steps. To automate the calculation, ChemCad is coupled to Excel by the DataMap feature of ChemCad. A VBA macro is used to control the simulation by detecting the fulfilment of termination criteria and updating the value of R and the setting of a divider at the end of the steps. The divider is used to switch between the accumulators. At each time step, the current values of R and divider setting are transferred to ChemCad, which then gives back selected results. To reduce the time requirement of the simulation, several measures are implemented. Since Step 0 has no optimisation variables, it is only simulated once; subsequent calculation starts from the end of Step 0. If at the end of Step 2 Constraints 2 or 3 are violated, the simulation is terminated. In Step 3, the B content of the main cut has a maximum value ($x_{mc,B,max}$) in time. If $x_{mc,B,max}$ does not reach 0.9952, the simulation is also terminated since the purity of the product will not be acceptable.

Performing the calculations in the original range results in a low number of points with acceptable purity. Model fitting to too few points might lead to low accuracy of the models. To avoid this, a second set of 500 points are generated by LHS on a narrower domain (Table 1) based on the points with acceptable purity. All the models are fitted by using the narrower domain.

Surrogate models are fitted by ALAMO to the results of the simulation necessary to calculate OF and the left-hand sides of Constraints 2 and 3: m_{fc1}, m_{mc}, t, $x_{fc2,B}$, $x_{fc2,C}$, $x_{fc2,E}$ and additionally to $x_{mc,B,max}$. The latter value shows not only if Constraint 1 is violated (the product purity is unacceptable) but also the level of the violation. (The value of $x_{mc,B}$ is not suitable for this purpose.) Alternatively, it would also be possible to fit a SM directly to OF; however, this would reduce the level of insight that can be obtained by analysing the models and would likely lead to a less accurate model.

Table 2 – Powers allowed for the polynomial basis functions.

Dependent variable	Univariate	Binary product	Ternary product
m_{fc1}	2–5	1–3	1–2
m_{mc}	2–5	1–3	-
t	2–3	-	-
$x_{fc2,B}$	2–5	-	-
$x_{fc2,C}$	2–3	1–2	-
$x_{fc2,E}$	2–5	1–3	-
$x_{mc,B,max}$	2–5	1–3	-

The independent (optimisation) variables influencing each dependent one are the following ones. m_{fc1} is a function of only R_1 and Cr_1. The composition of Fore-cut 2 ($x_{fc2,B}$, $x_{fc2,C}$ and $x_{fc2,E}$) depends on R_1, R_2, Cr_1 and Cr_2. m_{mc}, $x_{mc,B,max}$ and t can be influenced by all the independent variables (R_1, R_2, R_3, and Cr_1, Cr_2).

ALAMO uses a machine learning-based approach to fit algebraic models by optimising a selected criterion describing the goodness of the fit. The models are generated as combinations of previously chosen basis functions, not necessarily used in the final model. Here, the Bayesian information criterion is selected as the measure of the goodness of the fit, which not only takes the model error into account but also penalises the model size to avoid overfitting. The basis functions allowed are constant terms, linear, logarithmic, and exponential functions, as well as polynomials of the variables and their binary and ternary products with powers shown in Table 2. Note that due to technical limitations, the adaptive sampling feature of ALAMO is not used here.

Optimisation is performed with SQP by using the NLPSolve function of Maple. The function takes as arguments the OF and (optionally) the optimisation constraints. Here, the bounds of the ranges of the independent variables were also given as constraints to avoid extrapolation. With the values of the independent variables obtained from the optimisation, a simulation is performed to verify the accuracy of SMs at the estimated optimum. Additionally, the gradient vector is calculated at the optimum determined by SMs. Simulations are performed following the direction of the gradient vector in order to verify whether it is possible to increase OF further by approaching the constraints more.

By the SMBO, it is possible to re-optimise OF by Maple for different price ranges of methanol, incineration and heating steam without performing additional simulations. Price ranges of these parameters are chosen as p_B: 0.40–0.60 $/kg (Methanex., 2022), p_{inc}: 0.21–0.51 $/kg and p_{st}: 50–70 $/t. Performing one optimisation calculation takes only a fraction of a second. The model accuracy is evaluated by comparing the OF value of SMs and the one obtained with simulation at the highest p_B, p_{inc} and p_{st} values. OF is also calculated for the different price values without optimisation in order to assess the benefits of re-optimisation.

Additional calculations are made to investigate whether it is possible to narrow the original ranges of the optimisation variables using a lower number of simulations than the 500

one used originally. By a 1st approach, simulation is performed at a lower number of points (250, 350 or 400) generated by LHS within the original ranges. Considering only the feasible points (where no constraints are violated), narrowed ranges are then proposed based on the minimum and maximum values of the parameters. By a 2nd approach, surrogate models are fitted to $x_{fc2,B}$, $x_{fc2,C}$ and $x_{fc2,E}$. In the optimum both Constraints 2 and 3 should be active, and the set of points where this is true can be estimated with the help of the models fitted. As the models contain four independent variables, this set is a two-dimensional plane in the space of optimisation variable. The narrowing of the range is first studied for the original 500 points by using Maple, where it is possible to visually assess the R_1, Cr_1 and Cr_2 values where Constraint 2 and 3 are active. A three-dimensional space corresponds to an active Constraint 3. The values of R_1 and Cr_1 values at each point in this space determine R_2. The multicolour surfaces (Fig. 13) are the set of places where Constraints 2 is also active. The yellow and green surfaces correspond to the lower and upper bound of R_2. Only points between these surfaces should be taken into account to avoid extrapolation of the models. Subsequently, the narrowing is also studied for 250 points with a numerical method. A system of equations corresponding to active Constraints 2 and 3 is solved for R_1 and Cr_1 by substituting different values of R_2 and Cr_2 within their bounds in order to determine whether it is possible to narrow the range of R_1 and Cr_1.

4. Results

In this section, first fitting of SMs is presented, then the results of the SMBO are compared to those obtained by GA (Hegely and Lang, 2016) and the Nelder-Mead simplex (Hegely, 2023). After this, the process is re-optimised for different price values using the SMs, and finally, potential alternatives to the narrowing approach used here are discussed. The results are given with 3–4 valuable digits in order to show the sometimes slight differences between the results of the different methods, even though less precise values would be used in industrial practice.

4.1. Fitting of the surrogate models

From the original range (Table 1), all the data points can be used for model fitting for m_{fc1}, $x_{fc2,B}$, $x_{fc2,C}$ and $x_{fc2,E}$. However, only 51 calculations do not violate Constraints 2 or 3 and thus can be used for fitting a model for $x_{mc,B,max}$. More importantly, there are only 18 feasible points where the product purity is acceptable and that can be used for model fitting for m_{mc} and t. The highest OF value is 429.6 $ (Table 3), which can be considered as the result of using LHS as a random search optimisation method. The values of the optimisation variables and the simulation results are given for all the points in Hegely et al. (2023).

By using the narrowed range, the number of feasible points increased from 18 to 46, which is deemed to be sufficient. The number of points that can be used for fitting a model for $x_{mc,B,max}$ increased slightly to 56. At the best point, OF equals 480.7 $ (Table 3), and the $x_{fc2,C}/x_{fc2,B}$ and $x_{fc2,E}/x_{fc2,B}$ ratios are close to their limiting values. The detailed data of all points are also given in Hegely et al. (2023). Compared to the best point in the original range, Cr_1 increased considerably, which decreased the cost of incineration. A significant increase in R_3 also contributed to the profit, while R_2 and Cr_2 decreased.

Table 3 – Results of LHS as a random search optimisation method.

Optimisation variable	Original range	Narrowed range
R_1	5.77	5.80
R_2	3.23	2.13
R_3	2.62	3.22
Cr_1	0.1483	0.2168
Cr_2	0.0286	0.0241
Constraints		
$x_{fc2,C}/x_{fc2,B}$	0.0853	0.1026
$x_{fc2,E}/x_{fc2,B}$	0.0959	0.1170
Profit (OF) and its elements		
Income, $	2547	2522
Incineration cost, $	526	452
Steam cost, $	1591	1589
Profit (OF), $	429.6	480.7

The SMs used for optimisation are fitted on the narrowed ranges. The size of the models were between 7 ($x_{fc2,B}$) and 25 ($x_{fc2,C}$). Interestingly, Cr_2 does not influence the distillation time:

$$t = 95.93 \cdot R_1 + 16.04 \cdot R_2 + 78.61 \cdot \ln R_2 - 0.89 \cdot e^{R_3} + 939.52 \cdot e^{Cr_1} - 3,59 \cdot R_1^2 + 24.95 \cdot R_3^2 - 4531 \cdot Cr_1^2 \quad (2)$$

By increasing Cr_2, the duration of Step 2 decreases (less Fore-cut 2 is taken), but that of Step 3 is likely to increase to a very similar extent. As it is shown in Fig. 3, the surrogate model (surface) was able to predict the mass of Fore-cut 1 (dots) with good accuracy. On the increase of R_1, m_{fc1} decreases at low Cr_1 values but increases slightly at higher Cr_1 values. On the increase of Cr_1, m_{fc1} decreases since Step 1 is stopped earlier. The rest of the models are given in the Supporting information.

4.2. Results of the surrogate model-based optimisation

The results of SMBO are given in Table 4. In the optimum, both Constraints 2 and 3 are active, as expected. The results of the simulation and the SMs are very close to each other: the difference in OF is 2.6 $ (0.53%). The difference is in the same order of magnitude (in absolute values) for each element of the profit. By the simulation, the constraints are fulfilled, but the concentration ratios are also very close to the constraints, with the higher deviation being only 0.57% for $x_{fc2,E}/x_{fc2,B}$.

Comparing the simulation result to the optimum found by Hegely and Lang (2016) by GA, SMBO gives a 5.0% higher profit. Moreover, GA required 3000 simulations instead of 1000 by the present method. (Note that the total calculation time is approximately proportional to the number of simulations.) The suboptimality of the GA result is hinted at by the significant distance of $x_{fc2,C}/x_{fc2,B}$ from the limit of Constraint 2. R_1 decreased by 8.7%, whereas R_3 and Cr_2 changed only slightly. R_2 decreased by 19%. Cr_1 increased by 22%, thereby reducing the cost of incineration. The mass of the main cut, and thus the income decreased slightly (by 2.5%); however, the steam cost also decreased (by 3.1%) due to the lower reflux ratios. It must also be noted that, in the narrowed ranges, a higher OF value than that of GA is already obtained by LHS only.

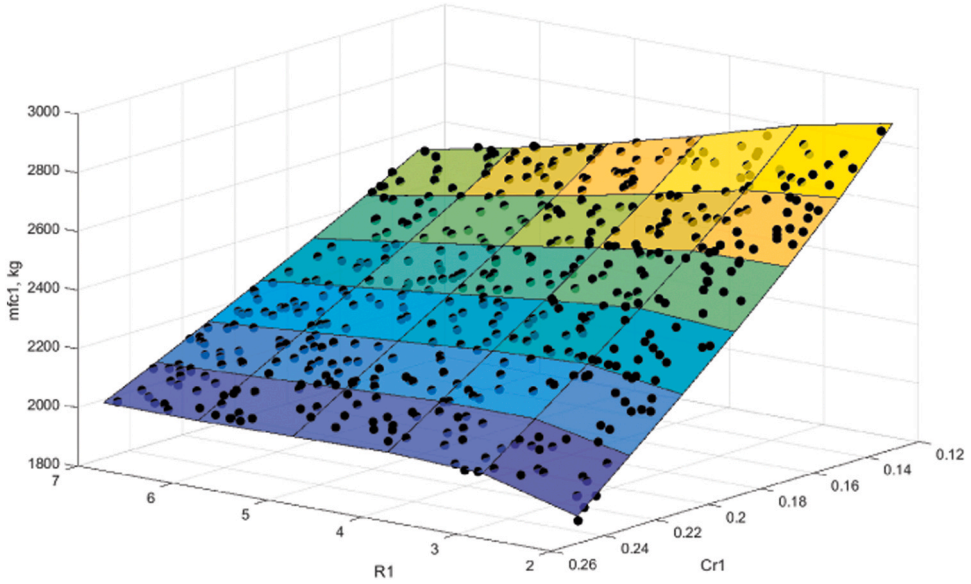

Fig. 3 – Mass of Fore-cut 1 calculated by simulation (dots) and by the surrogate model fitted (surface).

Table 4 – Comparison of the results of the surrogate model-based optimisation with those of GA (Hegely and Lang, 2016) and simplex (Hegely, 2023).

Optimisation variable	GA	Simplex	SMBO		Difference, %	
					SMBO to GA	SMBO to simplex
R_1	6.22	5.55	5.68		-8.68	+2.34
R_2	3.07	2.69	2.49		-18.8	-7.43
R_3	3.05	3.17	3.09		+1.31	-2.52
Cr_1	0.175	0.2012	0.2138		+22.2	+6.26
Cr_2	0.0262	0.0275	0.0255		-2.67	-7.27
Constraints			Model	Simulation		
$x_{fc2,C}/x_{fc2,B}$	0.0951	0.1058	0.1070	0.1064	+11.9	+0.57
$x_{fc2,F}/x_{fc2,B}$	0.1191	0.1182	0.1200	0.1198	+0.588	+1.35
Profit (OF) and its elements			Model	Simulation		
Income, $	2597	2563	2534	2533	-2.46	-1.17
Incineration cost, $	492	469	456	454	-7.72	-3.20
Steam cost, $	1638	1602	1585	1588	-3.05	-0.87
Profit (OF), $	467	493	493.0	490.4	+5.01	-0.53

By the SMBO technique, the values of OF and its elements are similar to the best one obtained by the Nelder-Mead simplex method (Hegely, 2023): OF is only by 0.5% lower. However, the number of simulations is higher (1000 instead of 236). R_2 and Cr_2 are lower by 7.4% and 7.3%, respectively, while Cr_1 is higher by 6.26%. The SMBO method is thus able to find the same OF value as the best one previously obtained. Even though the number of simulations of SMBO is higher than that of the simplex, the simplex is a local method, and it might converge to local optima or stop prematurely when reaching a constraint.

Since SMs are explicitly known, a more detailed analysis of the optimization problem is possible. To study the interaction between the variables related to Fore-cut 1, a contour plot of OF with R_1 and Cr_1 as independent variables is drawn (Fig. 4a; all other variables take their optimal value). Either Constraint 2 (green line) or Constraint 3 (blue line) are violated outside the shaded area. As in the optimum, both constraints are active, the corresponding contour line and the constraint lines intersect at one point. By increasing R_1, Cr_1 must be decreased (more Fore-cut 1 must be taken) to keep OF constant (except at high R_1 values for low OF). The maximum possible Cr_1 value is determined by Constraint 2 below the optimal R_1 and by Constraint 3 above it. On the other hand, by increasing R_2, Cr_2 has a minimum (for a given OF value) but changes only slightly (Fig. 4b). The maximum Cr_2 value is determined by Constraint 3 below the optimal R_2 and by Constraint 2 above. The ranges of acceptable R_2 and Cr_2 values are narrower than those of R_1 and Cr_1.

Although OF is a five-variable function, visualising the optimum is still possible. As mentioned earlier, an active Constraint 3 corresponds to the three-dimensional space shown in Fig. 5. In each point of this space, R_2 is determined by the values of R_1, Cr_1 and Cr_2. The set of points where Constraint 2 is also active is the multicolour surfaces on which the optimum (red dot) is located. At lower R_1 values, Constraint 2 is violated. Points below the yellow surface correspond to R_2 values outside the range used for model fitting and thus represent an extrapolation of the models that should be avoided.

The gradient of the objective function calculated from the SMs at the optimum is (17.2, 10.8, $-2.3 \cdot 10^{-6}$, 913, 4017), meaning that OF is most sensitive to Cr_2 and least sensitive to R_3. Since, by the simulation, the constraints are not active,

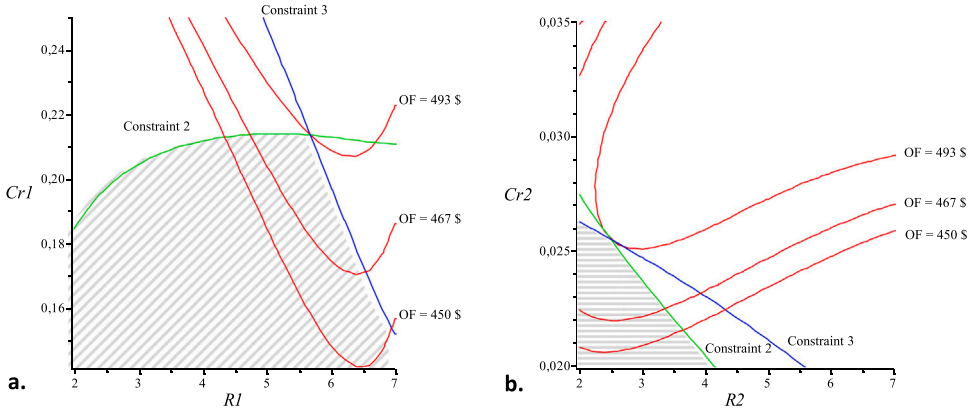

Fig. 4 – Contour plot of OF (red lines) with a. R_1 and Cr_1 and b. R_2 and Cr_2 as independent variables. Constraint 2 is shown as a green line, Constraint 3 as a blue one.

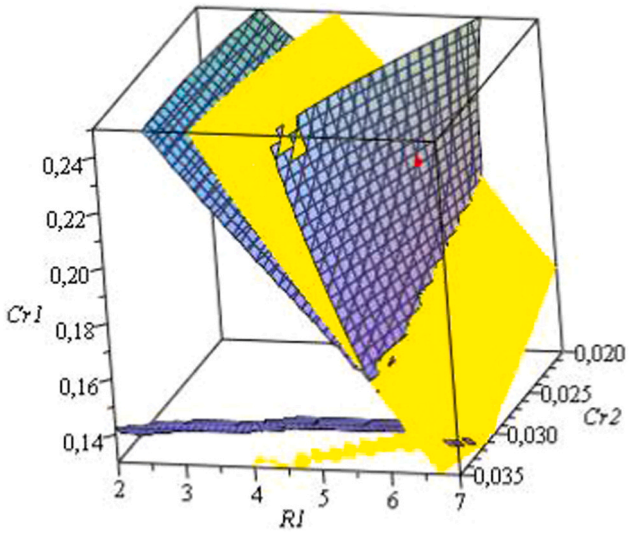

Fig. 5 – Plot of the active constraints (multicolour surfaces), the limit of surrogate model validity (yellow surface) and the optimum obtained from the surrogate models (red dot).

it is likely that OF can be further increased by approaching the constraints better. To follow the direction of the gradient, Cr_2 must be increased, which decreases the duration of Step 2. Even if the duration decreases by one time step (2 min), the constraints are violated; thus, it was not possible to further increase OF.

4.3. *Results of the re-optimisation*

The influence of methanol price on the OF and the optimal values of operational parameters is as follows. On the increase of p_B, Cr_1 decreases, while R_1 hardly changes (Fig. 6). More Fore-cut 1 is taken, which increases the cost of incineration. The mass of Fore-cut 2 decreases, to which the increase in Cr_2 also contributes. R_2 shows a considerable increase. R_3 and m_{mc} increase slightly. Due to the increase of m_{mc}, the profit becomes higher. When p_B increases from 0.46 to 0.60 $/kg, OF increases from 491 to 1277 $, and the duration of the process increases from 2080 to 2158 min

In the extreme case p_B= 0.60 $/kg, OF obtained from SMs and simulation is compared (Fig. 7) to determine the model error, which is low (1.6 $). OF is slightly underestimated by the SMs. OF is also calculated without optimisation for different p_B values. The difference between the OF obtained

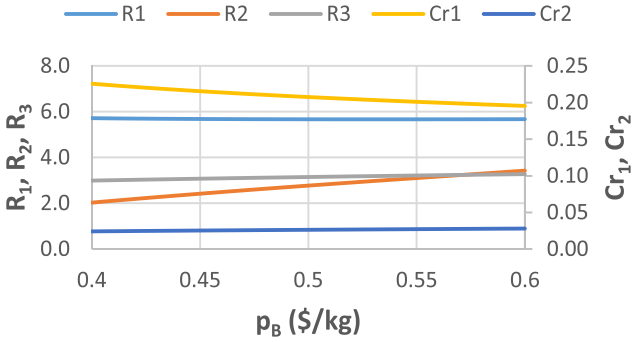

Fig. 6 – Influence of methanol price on the optimal values of operational parameters.

without and with re-optimisation is small, meaning that in this case, the operational parameters determined for a certain methanol price, even if they are not optimal anymore, can still be used if the price changes without a significant loss of profit.

On the increase of p_{inc}, Cr_1 and R_1 increase (Fig. 8). Less Fore-cut 1 is taken, which decreases the cost of incineration. On the other hand, more Fore-cut 2 is taken. R_2 decreases rapidly, and at p_{inc}= 0.32 $/kg, it reaches the lower bound of its range. Above this, the optimal R_2 is lower than its lower bound, but it is kept constant to avoid extrapolation. Decreasing R_2 is likely necessary in order not to violate Constraints 2 and 3 while less C and E are removed with Fore-cut 1. Cr_2 decreases only slightly, while R_3 (and thus m_{mc}) is almost constant.

Due to the increase of p_{inc}, the profit becomes lower even though less Fore-cut 1 is taken. When p_{inc} increases from 0.21 to 0.51 $/kg, OF decreases from 491 to −186 $. The duration of the process decreases from 2080 to 2040 min. Above p_{inc}= 0.44 $/kg, the operation is no longer economical.

The model error at the highest p_{inc} value (Fig. 9) is more important (–53.1 $) than in the case of varying p_B. OF is overestimated by the SMs. Although the difference between the OF values obtained without and with re-optimisation is slightly higher than in the case of varying p_B, re-optimisation does not have a significant impact.

On the increase of p_{st}, the decrease of the average reflux ratio of the process is expected. R_1 hardly changes (Fig. 10). The change in R_2 is the most important, although it is still not very high. R_3 (and thus m_{mc}) decreases slightly. Cr_1 increases slightly, as well, which decreases the amount of Fore-cut 1 taken. Cr_2 is almost constant. OF decreases from 491 to 106 $

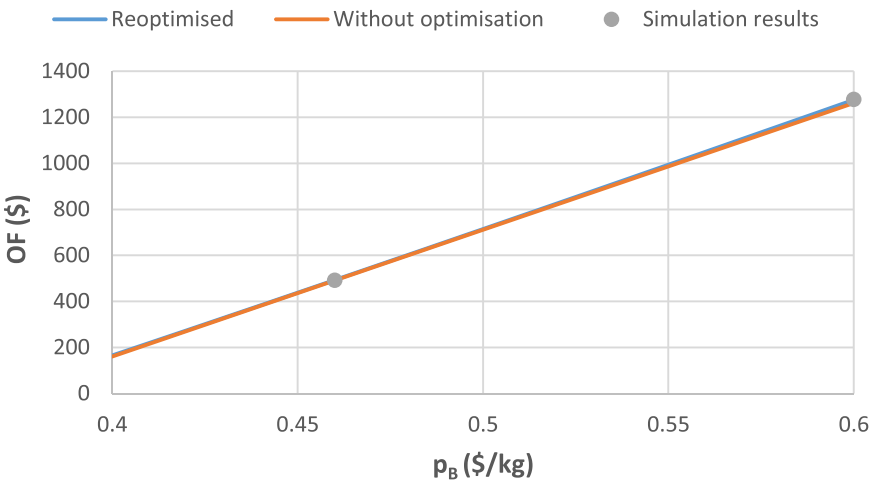

Fig. 7 – Influence of methanol price on the objective function.

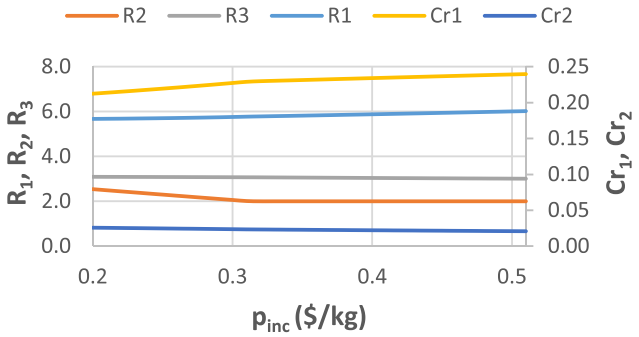

Fig. 8 – Influence of price of incineration on the optimal values of operational parameters.

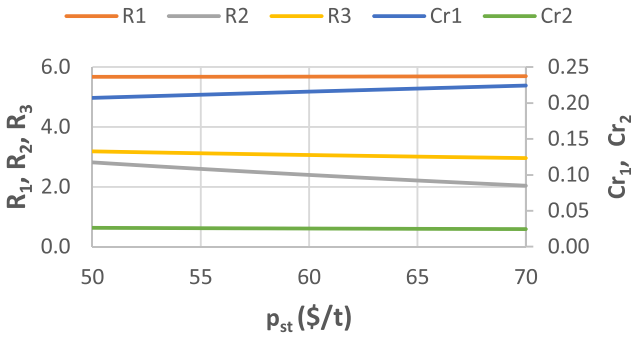

Fig. 10 – Influence of price of steam on the optimal values of operational parameters.

when p_{st} increases from 57.6 to 70 $/t. The duration of the process decreases from 2080 to 2034 min

The model error at the highest p_{st} value (–49.8) (Fig. 11) is similar to the one in the case of p_{inc}, and it is larger than in the case of varying p_B. Once again, the difference between the OF obtained without and with re-optimisation is small.

4.4. *Results of narrowing of the ranges*

By the first approach, several ranges are studied for different numbers of points (250, 350, 400). The ranges obtained are shown in Fig. 12, which includes the potential narrowed ranges based on the original 500 points and the narrowed ranges finally used for model fitting ("used"). Using less than 500 points always results in narrower ranges (except for R_3), but no clear conclusions can be drawn for the number of points to be used. The width of the final range is sometimes lower (R_2, Cr_2) but often similar to those obtained for 250–400 points. The optimum value of Cr_1 is outside the narrowed range for two out of four cases.

There are two different methods of the 2nd approach, where the narrowing of ranges is studied for 250 and 500

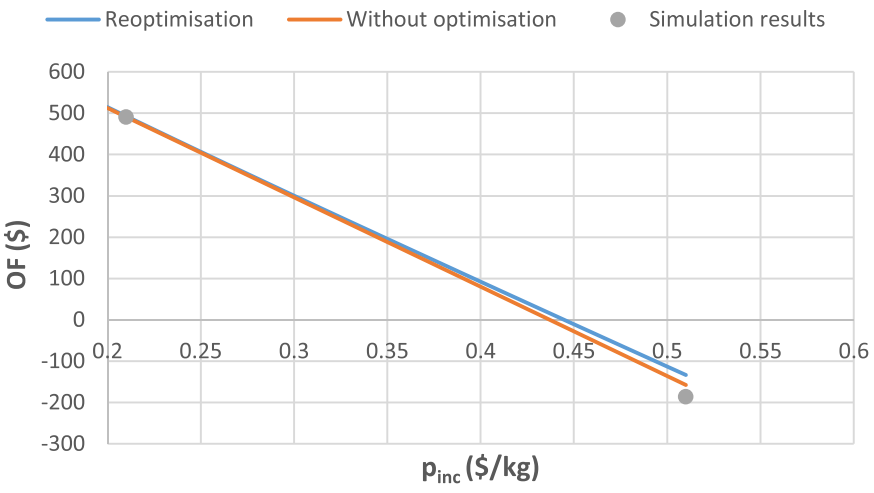

Fig. 9 – Influence of price of incineration on the objective function.

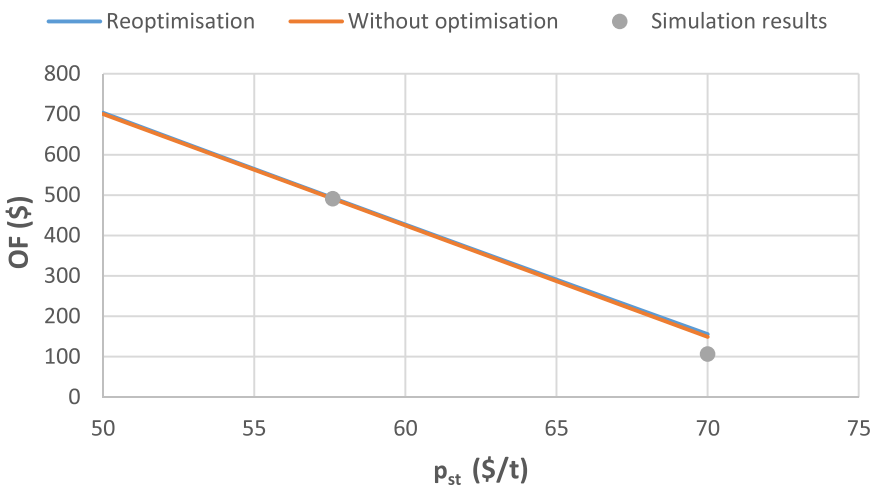

Fig. 11 – Influence of price of steam on the objective function.

points. By the visual method (using 500 points), it is possible to narrow the range of R_1 from 1–10 to 4.5–6.3 (Figs. 12 and 13). Similarly to Fig. 5, the three-dimensional space depicted in Fig. 13 is defined by the active Constraint 3, where the values of R_1, Cr_1, and Cr_2 determine that of R_2 at each point. The multicolour surfaces represent the locations where Constraint 2 is also active. If R_1 values are low, Constraint 2 is not met. The points outside the region limited by the yellow

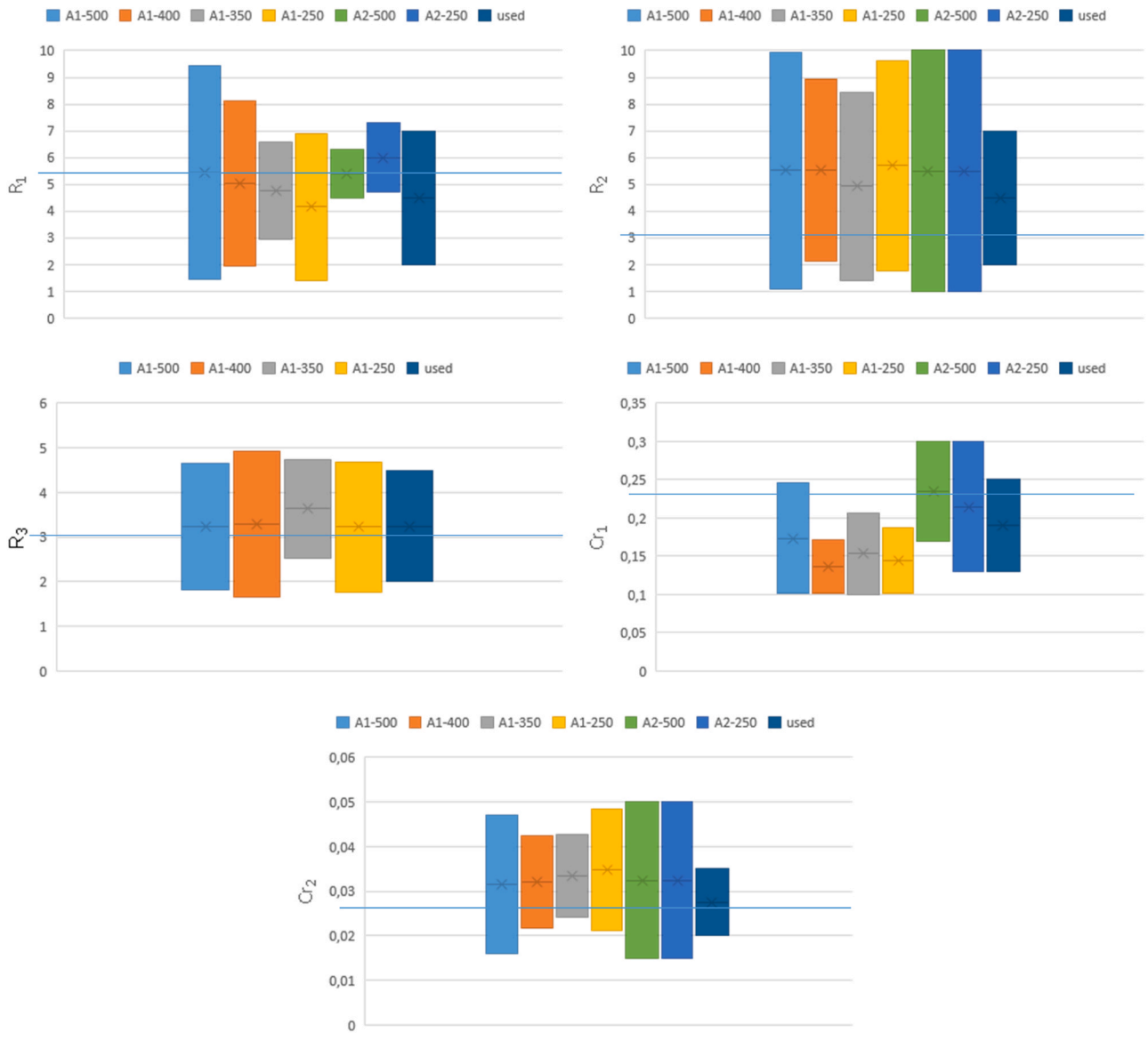

Fig. 12 – Narrowing the ranges of optimisation variables (A1: 1st approach A2: 2nd approach). The optimal values are shown with horizontal lines.

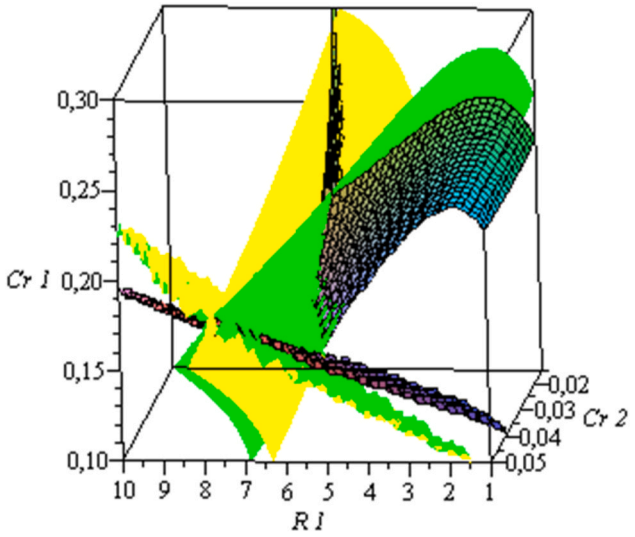

Fig. 13 – Plot of the set of points where Constraints 2 and 3 (multicolour surfaces) are active and limits of surrogate model validity (yellow and green surfaces) for models fitted to 500 sample points selected within the original range.

and green surfaces correspond to R_2 values that fall outside the range used for model fitting and should therefore be avoided as they represent an extrapolation of the models. The lower bound of Cr_1 can be increased from 0.10 to 0.17, but the upper bound cannot be changed. By the numerical method (using 250 points), the range of R_1 could be narrowed from 1–10 to 4.7-7.3. It is also possible to increase the lower bound of Cr_1 from 0.10 to 0.13. R_2 and Cr_2 could not be narrowed by either method of the 2nd approach. By using the 2nd approach, the optimum of Cr_1 is within the narrowed range. Therefore, for those variables (R_1 and Cr_1) where it is possible to determine a narrowed range with the 2nd approach, its use is recommended, while for the other variables, the 1st approach should be used. 250 points seem to be sufficient for the narrowing, meaning that SMBO could have been performed with 750 instead of 1000 simulations, provided the quality of the models does not deteriorate significantly.

5. Conclusions

A surrogate model-based method was proposed to reduce the computational intensity of the optimisation of batch distillation processes. The recovery of methanol from a five-component azeotropic waste solvent mixture was optimized. The objective function (OF) was the profit of a single batch, while constraints were given on the purity of the main cut and the composition of the recycled, 2nd fore-cut.

Dynamic simulations were performed by ChemCad in a set of points (generated by Latin hypercube sampling) in the space of optimisation variables (reflux ratios of the steps, stopping criteria of the two fore-cuts). Algebraic SMs were then fitted to the simulation results to describe OF and the constraints by the ALAMO machine learning technique. The resulting optimisation problem was solved very easily by SQP.

The surrogate models accurately described the results of the simulation. The profit obtained was by 5% higher than the one obtained by Hegely and Lang (2016) with a genetic algorithm, while the number of simulations was reduced from 3000 to 1000. The influence of the prices of methanol, incineration of the 1st fore-cut and heating steam on the OF and on the optimal values of operational parameters was studied by using SMs without new simulation. The difference between the profits obtained without and with re-optimisation was small (max. 3.9% of the total change in profit).

Future research will focus on evaluating the performance of the SM-based optimisation method for different distillation processes. Applying adaptive sampling will also be studied.

Declaration of Competing Interest

The authors declare that they have no known competing financial interests or personal relationships that could have appeared to influence the work reported in this paper.

Acknowledgements

The research was funded by the National Research, Development, and Innovation Fund of Hungary under Grants TKP2021-EGA-02, K-120083, FK-143059, by the János Bolyai Research Scholarship of the Hungarian Academy of Sciences, and by the ÚNKP-22-5-BME-325 New National Excellence Program of the Ministry for Culture and Innovation from the source of the National Research, Development and Innovation Fund. Ömer Faruk Karaman wishes to express his gratitude to the SH program for the support in this research.

Appendix A. Supporting information

Supplementary data associated with this article can be found in the online version at doi:10.1016/j.cherd.2023.02.043.

References

Cozad, A., Sahinidis, N.V., Miller, D.C., 2014. Learning surrogate models for simulation-based optimization. AIChE J. 60, 2211–2227. https://doi.org/10.1002/aic.14418

Esche, E., Weigert, J., Brand Rihm, G., Göbel, J., Repke, J., 2022. Architectures for neural networks as surrogates for dynamic systems in chemical engineering. Chem. Eng. Res. Des. 177, 184–199. https://doi.org/10.1016/j.cherd.2021.10.042

Furlonge, H.I., Pantelides, C.C., Sørensen, E., 1999. Optimal operation of multivessel batch distillation columns. AIChE J. 45 (4), 781–801. https://doi.org/10.1002/aic.690450413

Greaves, M.A., Mujtaba, I.M., Barolo, M., Trotta, A., Hussain, M.A., 2003. Neural-network approach to dynamic optimization of batch distillation: application to a middle-vessel column. Chem. Eng. Res. Des. 81, 393–401. https://doi.org/10.1205/02638760360596946

Hegely, L., 2023. Direct search methods for the fast optimisation of batch distillation processes. Sep. Purif. Technol. 306 Part A, 122448. https://doi.org/10.1016/j.seppur.2022.122448

Hegely, L., Lang, P., 2016. Optimization of a batch extractive distillation process with recycling off-cuts. J. Clean. Prod. 136, 99–110. https://doi.org/10.1016/j.jclepro.2016.04.140

Hegely, L., Karaman, Ö.F., Szucs, M.T., Lang, P., 2023. Latin hypercube sampling data for surrogate model-based optimisation of a batch distillation process. Mendeley Data V1. https://doi.org/10.17632/bh9xwnb6r9.1

Ibrahim, D., Jobson, M., Li, J., Guillén-Gosálbez, G., 2018. Optimization-based design of crude oil distillation units using surrogate column models and a support vector machine. Chem. Eng. Res. Des. 134, 212–225. https://doi.org/10.1016/j.cherd.2018.03.006

Jia, S., Qian, X., Yuan, X., 2017. Optimal design for dividing wall column using support vector machine and particle swarm

optimization. Chem. Eng. Res. Des. 125, 422–432. https://doi.org/10.1016/j.cherd.2017.07.028

Khazraee, S.M., Jahanmiri, A.H., Ghorayshi, S.A., 2011. Model reduction and optimization of reactive batch distillation based on the adaptive neuro-fuzzy inference system and differential evolution. Neural Comput. Appl. 20, 239–248. https://doi.org/10.1007/s00521-010-0364-x

Methanex, 2022. Methanex posts regional contract methanol prices for Europe, North America, Asia and China. https://www.methanex.com/our-business/pricing (accessed 13 October 2022).

Mujtaba, I.M., 2004. Batch distillation: design and operation. Imperial College Press, London, UK.

Mujtaba, I.M., Macchietto, S., 1993. Optimal operation of multicomponent batch distillation-multiperiod formulation and solution. Comput. Chem. Eng. 17 (12), 1191. https://doi.org/10.1016/0098-1354(93)80099-9

Mujtaba, I.M., Macchietto, S., 1997. Efficient optimization of batch distillation with chemical reaction using polynomial curve fitting techniques. Ind. Eng. Chem. Res. 36 (6), 2287–2295. https://doi.org/10.1021/ie960573d

Nemeth, B., Lang, P., Hegely, L., 2020. Optimisation of solvent recovery in two batch distillation columns of different size. J. Clean. Prod. 275, 122746. https://doi.org/10.1016/j.jclepro.2020.122746

Parhi, S.S., Rangaiah, G.P., Jana, A.K., 2020. Mixed-Integer dynamic optimization of conventional and vapor recompressed batch distillation for economic and environmental objectives. Chem. Eng. Res. Des. 154, 70–85. https://doi.org/10.1016/j.cherd.2019.12.006

Pommier, S., Massebeuf, S., Kotai, B., Lang, P., Olivier, B., Floquet, P., Gerbaud, V., 2008. Heterogeneous batch distillation processes: Real system optimisation. Chem. Eng. Process. 47, 408–419. https://doi.org/10.1016/j.cep.2007.01.022

Quirante, N., Javaloyes, J., Caballero, J.A., 2015. Rigorous design of distillation columns using surrogate models based on Kriging interpolation. AIChE J. 61, 2169–2187. https://doi.org/10.1002/aic.14798

Safe, M., Khazraee, S.M., Setoodeh, P., Jahanmiri, A.H., 2013. Model reduction and optimization of a reactive dividing wall batch distillation column inspired by response surface methodology and differential evolution. Math. Comput. Model Dyn. Syst. 19, 29–50. https://doi.org/10.1080/13873954.2012.691521

Viana, F.A.C., 2016. A tutorial on latin hypercube design of experiments. Qual. Reliab. Engng. Int. 32, 1975–1985. https://doi.org/10.1002/qre.1924

Wang, Y., Yang, X., Zhao, J., Liu, X., Yao, D., Cui, P., Wang, L., Zhu, Z., Li, X., Xu, D., 2020. Design and comprehensive analysis of a novel pressure-swing batch distillation process for the separation of a binary azeotrope with various boiling behaviors. Sep. Purif. Technol. 251, 117329. https://doi.org/10.1016/j.seppur.2020.117329

Williams, B., Cremaschi, S., 2021. Selection of surrogate modeling techniques for surface approximation and surrogate-based optimization. Chem. Eng. Res. Des. 170, 76–89. https://doi.org/10.1016/j.cherd.2021.03.028

Zhao, J., Shen, Y., Li, C., Zhao, F., Li, X., Zhu, Z., Wang, Y., Cui, P., Gao, J., 2021a. Sequential two-column batch distillation processes for separation of ternary mixture containing three binary minimum boiling point homoazeotropes. Sep. Purif. Technol. 270, 118826. https://doi.org/10.1016/j.seppur.2021.118826